Quantifying the accuracy of steady states obtained from the universal Lindblad equation

Frederik Nathan and Mark S. Rudner

Phys. Rev. B **109**, 205140 — Published 20 May 2024

DOI: 10.1103/PhysRevB.109.205140

Quantifying the accuracy of steady states obtained from the Universal Lindblad Equation

Frederik Nathan[1] and Mark S. Rudner[2]
[1] *Institute for Quantum Information and Matter, Caltech, Pasadena, California 91125, USA*
[2] *Department of Physics, University of Washington, Seattle, Washington 98195, USA*
(Dated: May 2, 2024)

We show that steady-state expectation values predicted by the universal Lindblad equation (ULE) are accurate up to bounded corrections that scale linearly with the effective system-bath coupling, Γ (second order in the microscopic coupling). We also identify a near-identity, quasilocal "memory-dressing" transformation, used during the derivation of the ULE, whose inverse can be applied to achieve *relative* deviations of observables that generically scale to zero with Γ, even for nonequilibrium currents whose steady-state values themselves scale to zero with Γ. This result provides a solution to recently identified limitations on the accuracy of Lindblad equations, which highlighted a potential for significant relative errors in currents of conserved quantities. The transformation we identify allows for high-fidelity computation of currents in the weak-coupling regime, ensuring thermodynamic consistency and local conservation laws, while retaining the stability and physicality of a Lindblad-form master equation.

The theoretical description of open quantum systems is an important problem in many fields of physics. While early groundwork was laid in the context of quantum optics and physical chemistry [1–6], recent advances in the control of complex quantum systems necessitate the development of new theoretical techniques [7–20].

In this work we focus on the broadly relevant Markovian regime which emerges for weak system-bath coupling relative to the intrinsic energy scales of the baths. In this context, Lindblad equations play a key role by providing the most general form of Markovian evolution that is guaranteed to preserve the physicality of solutions [21, 22]. Formulating incoherent evolution in terms of randomly timed "quantum jumps," Lindblad equations provide valuable physical insight and admit stable and relatively efficient numerical solutions via stochastic evolution of wave functions (rather than density matrices) [23, 24]. The latter feature allows Lindblad equations to be solved for systems of greater complexity than accessible with other approaches.

Historically, routes to deriving Lindblad equations from the evolution of a system coupled with its environment have relied on a rotating wave approximation (RWA), which assumes the spectral gaps of the system to be larger than any decoherence rate [5, 6]. While typically justified in the traditional contexts of quantum optics, the RWA is often not valid for complex quantum systems emerging in many fields of interest such as hybrid quantum systems [25], nonequilibrium many-body systems [26], and platforms for large-scale quantum simulation and information processing [27, 28].

Recently, several independent works discovered routes to circumvent the RWA [8, 13–15, 17, 19, 29], opening up many of the problems above for efficient study with Lindblad equations [8, 10–12, 29]. Particular applications include, e.g., bath-induced localization in driven many-body systems [30], modelling of qubit readout experiments [31, 32] and elucidating the conditions of validity for the Landau-Lifshitz-Gilbert equation [33]. In this work, we focus on the "Universal Lindblad Equation" (ULE), which was derived in Ref. [14] with rigorous bounds on approximation-induced errors; the bounds are controlled by the product of a characteristic effective system-bath coupling strength Γ (which is second-order in the microscopic system-bath coupling matrix elements), and a bath correlation time, τ [see Eq. (6)].

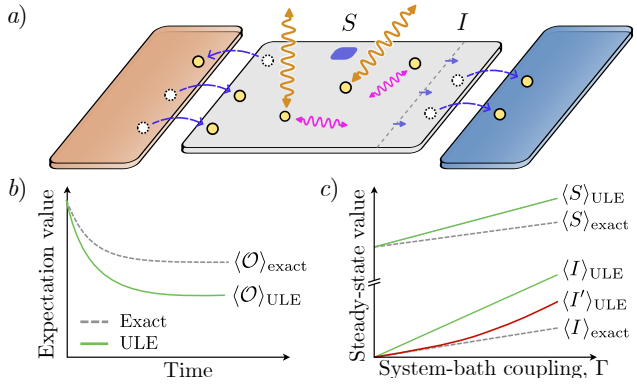

FIG. 1. (a) We consider an open quantum system (gray) coupled to one or more baths, such as, e.g., phonons/photons (purple/orange), or particle reservoirs (red/blue). We distinguish generic observables, S, such as particle or spin densities, from currents of conserved quantities, I. (b) The expectation value of any observable $\mathcal{O} = S, I$ generically converges to a unique value at long times, $\langle\mathcal{O}\rangle_{\text{exact}}$, regardless of initialization. (c) We show that the corresponding steady-state value resulting from the universal Lindblad equation (ULE), $\langle\mathcal{O}\rangle_{\text{ULE}}$, deviates from $\langle\mathcal{O}\rangle_{\text{exact}}$ by a value that scales to zero with the system-bath coupling, Γ. In the limit, $\Gamma \to 0$, the ULE hence accurately captures steady-state values that remain finite, as occurs for generic observables S. For nonequilibrium currents, I, whose steady-state values vanish in the limit $\Gamma \to 0$, an accurate steady-state value can be obtained from a "dressed" current I' that results from applying a near-identity, quasilocal transformation to I [Eqs. (10), (12)].

In parallel with the advances above, several groups recently explored the nontrivial tradeoffs of studying

nonequilibrium quantum systems with Lindblad equations. Even away from equilibrium, an open quantum system, e.g., as depicted in Fig. 1(a), generically converges to a unique *non-equilibrium steady state*, as schematically depicted for some given observable $\mathcal{O}$ by the dashed black curve in Fig. 1(b). The authors of Ref. [34] showed that the steady state of any Lindblad equation must deviate from the exact steady state by a correction linear in the effective system-bath coupling [the green curve in Fig. 1(b) depicts the flow of $\langle\mathcal{O}\rangle$ predicted by the ULE]. While the steady state of a Lindblad equation can approach the exact steady state in the weak-coupling limit, nonequilibrium currents such as, e.g., particle or heat currents, scale linearly with system-bath coupling. Consequently, their *relative deviations* generically remain finite as the coupling is taken to zero. This can lead to apparent violations of the second law of thermodynamics [8, 19] and local conservation laws [34].

To enable further progress in the field, here we quantify the fidelity of steady states resulting from the ULE, and demonstrate how the apparent inconsistencies above can be resolved. In Sec. I we summarize our main results. In Sec. II we review the problem addressed by our work: quantifying the accuracy of steady states of the ULE. In Sec. III we revisit the derivation and key features of the ULE relevant for the problem. In Sec. IV we present our solution via rigorous bounds on the deviations of observables computed with the ULE steady state compared with those obtained from the exact steady state. In Sec. V we demonstrate our results in numerical simulations of magnon transport in a spin chain. We conclude with a discussion in Sec. VI. Details of derivations and supplemental data are provided in Appendices.

I. SUMMARY OF MAIN RESULTS

We report two main results, summarized in Fig. 1(c):

1. First, we show that in the limit $\Gamma\tau \to 0$ the ULE faithfully captures the steady-state values of generic observables in *absolute* scale: for a generic observable, the steady-state value predicted by the ULE deviates from the true steady-state value by an amount that scales to zero with $\Gamma\tau$ [Eq. (15)].

2. Second, we demonstrate that steady-state expectation values with vanishing *relative* deviations in the limit $\Gamma\tau \to 0$ can be obtained by applying the inverse of a quasilocal, near-identity "memory-dressing" transformation that was employed to obtain the ULE [14] [see Eqs. (10) and (12) below]. The transformation only affects observables with support near regions connected to baths. This result enables the computation of accurate and thermodynamically-consistent nonequilibrium currents which obey local conservation laws. Our analysis is supported by numerical simulations (Fig. 2).

Before embarking on the technical discussion, we offer a few clarifying remarks about the nature of our results.

Firstly, we emphasize that the memory dressing transformation can be neglected for many applications: it is only required for computing nonequilibrium currents (or other quantities whose steady-state values vanish in the weak-coupling limit) with support close to points of contact with baths. The transformation is *not* needed for quantities with finite steady-state values in the weak-coupling limit, such as, e.g., spin or occupancy distributions.

Secondly, our results establish that the ULE provides significant practical advantages over the Bloch Redfield equation (BRE), both with and without the memory dressing transformation: as a Lindblad equation, the ULE provides a stable, positivity preserving map for the evolution of an open quantum system's density matrix. The ULE can therefore be used to study evolution and steady states of open quantum systems using stochastic wave function evolution approaches. Being computationally less costly than the density matrix evolution of the BRE, stochastic wave function evolution allows much more complex quantum systems to be systematically studied [**?**], including many body systems. See, e.g., Refs. [30–33] for examples of applications.

After a steady state is computed from the ULE, the inverse of the memory dressing transformation can be applied if one needs to compute nonequilibrium currents near points of contact with baths—otherwise, the transformation provides a negligible correction to the steady-state value of the observable in question. Applying the transformation has the same computational complexity as evaluating the Bloch-Redfield dissipator one time. While the memory dressing transformation breaks the positivity of the density matrix, it does so *in a small and controlled way, bounded by* $\Gamma\tau$, which systematically brings associated observables *closer* to their true values. Since the transformation is applied *after* the evolution, the stability of the Lindblad evolution and applicability of quantum trajectory approaches are therefore retained.

II. FORMULATION OF PROBLEM

We consider a quantum system with Hamiltonian $H_{\mathcal{S}}$, where one or more degrees of freedom $\{X_\alpha\}$ are coupled to degrees of freedom in the surrounding environment, or "bath," $\{B_\alpha\}$, such as, e.g., photonic or phononic modes, or creation/annihilation operators of particles in attached reservoirs [see Fig. 1(a)]. The environment can, e.g., consist of several baths out of mutual equilibrium, where different subsets of $\{B_\alpha\}$ act on distinct baths. The combined system has Hamiltonian

$$H_{\mathcal{SB}} = H_{\mathcal{S}} + H_{\mathcal{B}} + \sqrt{\gamma}\sum_{\alpha=1}^{N} X_\alpha B_\alpha, \tag{1}$$

where $H_{\mathcal{B}}$ is the Hamiltonian of the bath, and we introduced γ as a redundant energy scale parameterizing the system-bath coupling strength. We take each X_α to have unit spectral norm and take the environment to be in a state where each B_α has expectation value zero [35].

We consider the broadly relevant case where the environment is Gaussian (e.g., comprised of free bosonic or fermionic modes). A Gaussian environment is fully characterized by its two-point correlation function $J_{\alpha\beta}(t) = \langle B_\alpha(t) B_\beta(0)\rangle$ with $B_\alpha(t) \equiv e^{iH_{\mathcal{B}}t} B_\alpha e^{-iH_{\mathcal{B}}t}$. Our discussion considers two additional objects which equivalently encode the properties of the environment: the bath spectral function, $J_{\alpha\beta}(\omega) \equiv \int \frac{dt}{2\pi} e^{-i\omega t} J_{\alpha\beta}(t)$, and the "jump correlator" $g_{\alpha\beta}(t) = \int d\omega\, e^{-i\omega t} [\sqrt{J(\omega)/2\pi}]_{\alpha\beta}$, with $\sqrt{\cdot}$ denoting the matrix square root.

Observables of the system are determined by the reduced density matrix

$$\rho(t) = \mathrm{Tr}_{\mathcal{B}}[\rho_{\mathcal{SB}}(t)]. \tag{2}$$

Here $\rho_{\mathcal{SB}}(t)$ denotes the exact density matrix of the combined system, whose evolution is described by $\partial_t \rho_{\mathcal{SB}}(t) = -i[H_{\mathcal{SB}}, \rho_{\mathcal{SB}}(t)]$. For thermodynamically large environments, $\rho(t)$ generically goes to a unique steady state in the long-time limit regardless of the initial state of the system, ρ_0 [36]:

$$\bar{\rho}_{\mathrm{exact}} \equiv \lim_{t\to\infty} \rho(t). \tag{3}$$

Away from equilibrium, $\bar{\rho}_{\mathrm{exact}}$ depends on the details of the environment and the system-bath coupling. Such nonequilibrium steady states can be found by establishing approximate equations of motion for $\rho(t)$ and seeking their steady state solutions.

In the regime where the effective system-bath coupling is small relative to the inverse correlation time of the bath, it was recently shown that the system's evolution is well-described by the ULE [14, 15, 29]:

$$\partial_t \rho \approx i[\rho, H_{\mathcal{S}} + H_{\mathrm{LS}}] + \sum_{\alpha=1}^{N} \left(L_\alpha \rho L_\alpha^\dagger - \tfrac{1}{2}\{L_\alpha^\dagger L_\alpha, \rho\}\right), \tag{4}$$

where $L_\alpha = \sum_{mn\beta} [\sqrt{2\pi\gamma J(E_m - E_n)}]_{\alpha\beta} |m\rangle\langle m| X_\beta |n\rangle\langle n|$ with $H_{\mathcal{S}}|n\rangle = E_n|n\rangle$. The Hermitian Lamb shift H_{LS} effectively renormalizes $H_{\mathcal{S}}$; its form is given in Ref. [14]. Our goal is to characterize the fidelity of the steady state of the ULE,

$$\bar{\rho}_{\mathrm{ULE}} \equiv \lim_{t\to\infty} e^{\mathcal{L}_{\mathrm{ULE}} t}[\rho_0]. \tag{5}$$

Here $\mathcal{L}_{\mathrm{ULE}}$ denotes the ULE Liouvillian, whose action on an arbitrary density matrix ρ is given by the right-hand side of Eq. (4). Note that $\mathcal{L}_{\mathrm{ULE}}[\bar{\rho}_{\mathrm{ULE}}] = 0$.

III. REVIEW OF THE ULE

We first review the key features of the ULE [14].

A. Derivation of the ULE

The validity of the ULE is controlled by two timescales, Γ^{-1} and τ, given by

$$\Gamma = 4\gamma \left[\int_{-\infty}^{\infty} dt\, \|g(t)\|_{2,1}\right]^2, \quad \tau = \frac{\int_{-\infty}^{\infty} dt\, \|g(t)t\|_{2,1}}{\int_{-\infty}^{\infty} dt\, \|g(t)\|_{2,1}}, \tag{6}$$

where $\|g\|_{2,1} \equiv \sum_\beta (\sum_\alpha |g_{\alpha\beta}|^2)^{1/2}$. The rate Γ bounds the exact rate of evolution induced by the bath: $\|\partial_t\rho - i[\rho, H_S]\| \le \Gamma/2$, where $\|\cdot\|$ denotes the trace norm [14, 37]. The timescale τ is a characteristic correlation time of the bath; the dimensionless number $\Gamma\tau$ controls the approximations involved in deriving the ULE (as well as the Bloch-Redfield equation [13, 14]).

To derive the ULE, starting from Eq. (2) we first expand $\partial_t\rho$ to leading order in γ, yielding $\partial_t\rho(t) = \mathcal{L}_{\mathrm{BR}}[\rho(t)] + \xi_{\mathrm{BR}}(t)$ [4, 13, 14], where $\mathcal{L}_{\mathrm{BR}}$ denotes the Bloch-Redfield (BR) Liouvillian [38]. The residual $\xi_{\mathrm{BR}}(t)$ captures the difference between the exact value of $\partial_t\rho$ and that resulting from the BR equation [14]. Refs. [13, 14] recently established that $\|\xi_{\mathrm{BR}}(t)\| \le 2\Gamma^2\tau$ [37].

We obtain the ULE by transforming to a weakly "memory-dressed" frame of operator space using a near-identity quasilocal superoperator, $\mathcal{V}$:

$$\rho' = \mathcal{V}[\rho]. \tag{7}$$

We provide an explicit expression for $\mathcal{V}$ in Eq. (10) below. By design, $\mathcal{V}$ preserves the Hermiticity and trace of ρ, and satisfies $-i[\mathcal{V}, \mathcal{H}_{\mathcal{S}}] = \mathcal{L}_{\mathrm{ULE}} - \mathcal{L}_{\mathrm{BR}}$ [14], where $\mathcal{H}_{\mathcal{S}}[\rho] \equiv [H_S, \rho]$. Evaluating $\partial_t\rho'(t)$ gives

$$\partial_t\rho'(t) = \mathcal{L}_{\mathrm{ULE}}[\rho'(t)] + \xi(t), \tag{8}$$

where the residual $\xi(t)$ satisfies $\|\xi(t)\| \le 2\Gamma^2\tau$ [39]. The ULE is obtained by neglecting $\xi(t)$, which is subleading in $\Gamma\tau$, since $\mathcal{L}_{\mathrm{ULE}}$ consists of terms of order Γ and Γ^0.

Ref. [14] showed that $\|\mathcal{V} - \mathbf{1}\|_{\mathrm{SO}} \le \Gamma\tau$, where $\|\mathcal{A}\|_{\mathrm{SO}} = \sup_{\mathcal{O}} \|\mathcal{A}[\mathcal{O}]\|/\|\mathcal{O}\|$. As a result, ρ and ρ' nearly coincide when $\Gamma\tau \ll 1$:

$$\|\rho' - \rho\| \le \Gamma\tau. \tag{9}$$

Note that both $\|\rho - \rho'\| \ll 1$ and ξ are negligible in the limit $\Gamma\tau \ll 1$. In this sense, the ULE is accurate when $\Gamma\tau \ll 1$.

B. Memory-dressing transformation

The transformation to the memory-dressed frame, $\mathcal{V}$, is given by $\mathbf{1} + \delta\mathcal{V}$, with

$$\delta\mathcal{V}[\rho] = \gamma \int_{-\infty}^{\infty} dt dt' [\tilde{X}_\alpha(t), \rho \tilde{X}_\beta(t')] f_{\alpha\beta}(t, t') + \mathrm{h.c.}, \tag{10}$$

where $\tilde{X}_\alpha(t) = e^{iH_{\mathcal{S}}t} X_\alpha e^{-iH_{\mathcal{S}}t}$, the indices α and β are implicitly summed over, and $f_{\alpha\beta}(t,t') \equiv \sum_\lambda \int_{-\infty}^{\infty} ds\, g^*_{\alpha\lambda}(t-s) g^*_{\lambda\beta}(s-t') \theta(t-t')[\theta(t) - \theta(s)]$. In

App. A we provide alternative expressions for $\mathcal{V}$ in terms of the eigenstates of $H_\mathcal{S}$, and via an iterative expansion. Whereas the standard Markov approximation made en route to the Bloch-Redfield equation [6] amounts to approximating the density matrix as constant within the brief window of nonzero bath-correlations, passing to the memory-dressed frame effectively incorporates a more intricate averaging of the density matrix over the window of decaying correlations in the bath.

The memory frame transformation $\mathcal{V}$ can be shown to induce $O(\Gamma\tau)$ corrections to ρ, and can thus typically be ignored in the limit $\Gamma\tau \ll 1$ [14]. However, the corrections *are* relevant for observables whose steady-state values scale with Γ, such as nonequilibrium currents. We demonstrate below how to obtain negligible relative errors of these quantities by applying the inverse of the memory dressing transformation to the ULE steady state, i.e., by computing their expectation values with the operator $\mathcal{V}^{-1}[\bar{\rho}_{\rm ULE}]$. Using $\|\delta\mathcal{V}\|_{\rm SO} \leq \Gamma\tau$, Taylor expansion yields $\mathcal{V}^{-1} = 1 - \delta\mathcal{V} + \delta^{(2)}\mathcal{V}$, where, for $\Gamma\tau < 1$, $\|\delta^{(2)}\mathcal{V}\|_{\rm SO} \leq (\Gamma\tau)^2/(1-\Gamma\tau)$.

Importantly, $\mathcal{V}$ only affects observables with support near regions connected to baths: firstly, the integrand defining $f_{\alpha\beta}$ below Eq. (10) is nonzero only for $t > 0, s < 0$ and vice versa. For a bath with a smooth spectral function (i.e., finite memory), $g(t)$ decays to zero for large t [14] with a characteristic decay time τ_g. Hence, $f(t,t')$ also decays with a characteristic timescale of order τ_g for large $|t|$ or $|t'|$. Moreover, $\tilde{X}_\alpha(t)$ only has support within a distance $v_{\rm LR}t$ from the support of X_α, where $v_{\rm LR}$ denotes the system's Lieb-Robinson velocity. Thus, $\mathcal{V}$ only significantly affects operators with support within a distance $\ell_\mathcal{V} \sim v_{\rm LR}\tau_g$ from regions connected to baths.

IV. FIDELITY OF ULE STEADY STATE OBSERVABLES

Here we bound the differences between the exact steady-state value of a given observable, and the steady-state values resulting from the ULE with and without accounting for the memory-dressing transformation. In the following, we will use $\langle\mathcal{O}\rangle_{\rm exact}$ and $\langle\mathcal{O}\rangle_{\rm ULE}$ to denote expectation values of the observable $\mathcal{O}$ in the exact steady-state and the ULE steady state, respectively:

$$\langle\mathcal{O}\rangle_{\rm exact} \equiv {\rm Tr}[\bar{\rho}_{\rm exact}\mathcal{O}], \quad \langle\mathcal{O}\rangle_{\rm ULE} \equiv {\rm Tr}[\bar{\rho}_{\rm ULE}\mathcal{O}]. \tag{11}$$

To facilitate the comparison, we first translate $\langle\mathcal{O}\rangle_{\rm exact}$ to the memory-dressed frame via $\langle\mathcal{O}\rangle_{\rm exact} = {\rm Tr}[\mathcal{O}'\bar{\rho}'_{\rm exact}]$, where $\bar{\rho}'_{\rm exact} \equiv \mathcal{V}[\bar{\rho}_{\rm exact}]$, and [40]

$$\mathcal{O}' \equiv \mathcal{V}^{-1\dagger}[\mathcal{O}]. \tag{12}$$

Next, by setting $\partial_t\rho' = 0$ in Eq. (8), note that

$$\bar{\rho}'_{\rm exact} = \bar{\rho}_{\rm ULE} + \mathcal{L}_{\rm ULE}^{-1}[\bar{\xi}], \tag{13}$$

where $\bar{\xi} = \lim_{t\to\infty}\xi(t)$; see Appendix B for derivation. Combining these results with $\|\bar{\xi}\| \leq 2\Gamma^2\tau$, we conclude

$$|\langle\mathcal{O}'\rangle_{\rm ULE} - \langle\mathcal{O}\rangle_{\rm exact}| \leq C_\mathcal{O}\Gamma\tau|\langle\mathcal{O}'\rangle_{\rm ULE}|, \tag{14}$$

where $C_\mathcal{O} \equiv 2\Gamma\|\mathcal{L}_{\rm ULE}^{\dagger -1}[\mathcal{O}' - \langle\mathcal{O}'\rangle_{\rm ULE}]\|/|\langle\mathcal{O}'\rangle_{\rm ULE}|$. Crucially, as we show in Appendix C, $C_\mathcal{O}$ is finite for generic $\mathcal{O}$, and remains so as $\Gamma \to 0$, including for currents whose steady-state values scale to zero with Γ [41]. Thus, the relative deviation of $\langle\mathcal{O}'\rangle_{\rm ULE} = {\rm Tr}\{\mathcal{V}^{-1}[\bar{\rho}_{\rm ULE}]\mathcal{O}\}$ generically vanishes in the limit $\Gamma\tau \ll 1$.

The transformation to the memory-dressed frame can typically be neglected if $\mathcal{O}$ has a finite steady-state value in the limit $\Gamma\tau \ll 1$. Specifically, using Eq. (14) along with $|\langle\mathcal{O}'\rangle_{\rm ULE} - \langle\mathcal{O}\rangle_{\rm ULE}| \leq \frac{\Gamma\tau}{1-\Gamma\tau}\|\mathcal{O}\|_2$ (where $\|\cdot\|_2$ denotes the maximal singular value norm) [42] gives

$$|\langle\mathcal{O}\rangle_{\rm ULE} - \langle\mathcal{O}\rangle_{\rm exact}| \leq C_\mathcal{O}\Gamma\tau|\langle\mathcal{O}\rangle_{\rm ULE}| + \frac{\Gamma\tau + C_\mathcal{O}\Gamma^2\tau^2}{1-\Gamma\tau}\|\mathcal{O}\|_2. \tag{15}$$

The right hand side of Eq. (15) scales to zero when $\Gamma\tau \to 0$, implying that the absolute deviation of $\langle\mathcal{O}\rangle_{\rm ULE}$ vanishes in this limit. The magnitude of the correction from the memory-dressing transformation (second term above) moreover decays to zero with the distance from $\mathcal{O}$ to the bath, over the characteristic scale $\ell_\mathcal{V}$, due to the quasilocality of $\mathcal{V}$. Thus, in the weak-coupling limit, the correction from $\mathcal{V}$ is only relevant if $\lim_{\gamma\to 0}\mathcal{O} = 0$ *and* $\mathcal{O}$ has support within a distance $\ell_\mathcal{V}$ from regions connected to baths.

Equations (14) and (15) are our main results: Eq. (15) demonstrates that steady-state expectation values of observables computed from the ULE have vanishing *absolute* deviations from their exact counterparts in the weak-coupling limit. Equation (14) shows that ULE steady-state observables are guaranteed to have vanishing *relative* deviations when the transformation to the memory-dressed frame is accounted for by using the memory-dressed observable, $\langle\mathcal{O}'\rangle_{\rm ULE} = {\rm Tr}[\bar{\rho}_{\rm ULE}\mathcal{O}']$, rather than the bare observable, $\langle\mathcal{O}\rangle_{\rm ULE} = {\rm Tr}[\bar{\rho}_{\rm ULE}\mathcal{O}]$. We emphasize that the bounds in Eqs. (14) and (15) are loose, and define "worst case" deviations. We expect that actual deviations can often be much smaller.

V. NUMERICAL DEMONSTRATION

We demonstrate our results in simulations of magnon transport in a spin chain. We consider a chain of 9 sites with Hamiltonian $H_\mathcal{S} = \sum_{n=1}^{8} g(\sigma_n^x\sigma_{n+1}^x + \sigma_n^y\sigma_{n+1}^y + \Delta\sigma_n^z\sigma_{n+1}^z) + \sum_{n=1}^{9} h_n\sigma_n^z$, where σ_n^α is the $\alpha = \{x,y,z\}$ Pauli operator on spin n; the same model was studied in Ref. [34]. We couple σ_1^x and σ_9^x to two Gaussian baths through the terms $\sqrt{\gamma}\sigma_1^x B_1 + \sqrt{\gamma}\sigma_9^x B_2$. The baths are Ohmic, with temperatures T_1 and T_2. The bath spectral function reads $J_{\alpha\beta}(\omega) = \delta_{\alpha\beta}\frac{\omega e^{-\omega^2/\Lambda^2}}{\omega_0} n_{\rm B}(\omega/k_{\rm B}T_\alpha)$, with $\delta_{\alpha\beta}$ the Kronecker delta, ω_0 a normalizing frequency, Λ a high-frequency cutoff, $n_{\rm B}$ the Bose-Einstein distribution, and $k_{\rm B}$ the Boltzmann constant. We simulate the model with $k_{\rm B}T_1 = g$, $k_{\rm B}T_2 = 6g$, $\Delta = 1.4g$, $\Lambda = 8g$, and $h_n = \frac{2}{3}(n-5)g$, describing a uniform field gradient.

The system's spectrum, $\{E_m - E_n\}$, has mean adjacent-value spacing $4.9\cdot 10^{-5}g$, while the mean decay rate prescribed by Fermi's golden rule is given

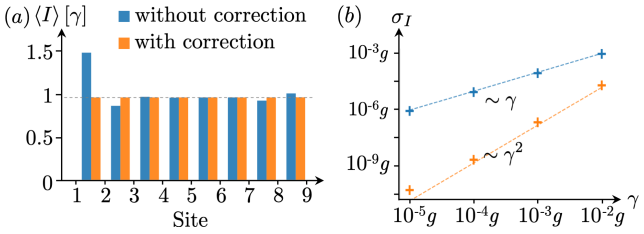

FIG. 2. Bare and dressed steady-state bond currents in a 9-site spin chain connected to two baths of unequal temperatures; see text for model details. (a) The bare bond currents vary significantly from site to site (blue bars), apparently violating current conservation. The dressed currents (orange bars) are near-uniform. Note the negligible effect of the memory dressing transformation deep in the bulk. (b) Scaling of the standard deviation of the bond currents in the 9 site chain, σ_I, as a function of γ (crosses).

by $\frac{2\pi\gamma}{D}\sum_{n,m=1}^{D}\left[J_1(E_n-E_m)|\langle n|\sigma_1^x|m\rangle|^2+J_2(E_n-E_m)|\langle n|\sigma_9^x|m\rangle|^2\right]\approx 23\gamma$, where $D=2^9$ is the system's Hilbert space dimension. The commonly used Davies equation [5, 43] (based on the RWA) is thus expected to be valid when $\gamma \ll 2.2\cdot 10^{-6}g$. On the other hand, explicit calculation shows $\Gamma\tau\approx 31\gamma/g$, implying that the approximations leading to the ULE are justified when $\gamma \ll 0.03g$.

Microscopically, the magnon current on the bond from site n to site $n+1$ is given by $I_{n+1,n}=(4ig\sigma_{n+1}^{+}\sigma_n^{-}+\text{h.c.})$. Since the exact evolution of the combined system yields $\partial_t\sigma_n^z = I_{n,n-1}-I_{n+1,n}$ for $1<n<9$, $\langle I_{n,n+1}\rangle_{\text{exact}}$ must be uniform throughout the system. On the other hand, $\langle I_{n+1,n}\rangle_{\text{ULE}}$ may be non-uniform near the baths, because the quasilocal Lamb shift and jump operators of the ULE modify the equation of motion for $\sigma_n^z(t)$. Non-trivially, Eq. (14) predicts that the *dressed* bond currents, $\langle I'_{n,n+1}\rangle_{\text{ULE}}$, are homogeneous throughout the system, up to relative deviations that scale to zero with γ. This feature thus serves as a consistency check of our analysis and indicator of the fidelity of the bond currents obtained with the ULE [44].

Fig. 2(a) shows the steady state values of $\{\langle I'_{n+1,n}\rangle_{\text{ULE}}\}$ and $\{\langle I_{n+1,n}\rangle_{\text{ULE}}\}$ [45], obtained for $\gamma=10^{-3}g$. Near-identical data are found for all probed values of γ smaller than $10^{-2}g$. Evidently, the bare currents exhibit significant non-uniformities near the ends of the chain, while the dressed currents are nearly uniform. These deviation are consistent with expected subleading $\mathcal{O}(\gamma^2)$ corrections: in Fig. 2b, we show the γ-scaling of the standard deviations of the bare and dressed current. While the standard deviation of the bare currents scales linearly with γ, that of the dressed currents scales *quadratically* with γ. Deep in the bulk, the bare and dressed bond currents in Fig. 2(a) are near-identical, indicating that the memory dressing transformation only affects observables in vicinities of baths. In Appendix D we provide data confirming that the memory dressing transformation is not needed to accurately capture the expectation values of $\{\sigma_n^z\}$, which remain finite when $\gamma\to 0$.

We finally bound the deviation of the magnon current precicted by the ULE via Eq. (14). We obtain $C_{I_{1,2}}\approx 1300$ for multiple values of γ between $10^{-5}g$ and $10^{-2}g$ (indicating that $\lim_{\gamma\to 0}C_{I_{1,2}}$ is finite), and $\Gamma\tau\approx 31\gamma/g$. Hence the current predicted by the ULE is *guaranteed* to be accurate (have relative deviation much smaller than 1) when $\gamma \ll 2.5\cdot 10^{-5}g$. We expect $\langle I'_{1,2}\rangle_{\text{ULE}}$ to be accurate for values of γ above this rigorous, but loose, bound: the standard deviation of the dressed bond currents is of order 1% even for $\gamma\approx 10^{-2}g$ [see Fig. 2(b)], suggesting that the corrected ULE observables may remain accurate up to this value.

VI. DISCUSSION

In this work, we established upper bounds on the steady-state deviations of observables computed from the ULE. Our analysis revealed two results: (1) We demonstrated that the ULE yields accurate steady-state values of observables in the weak-coupling limit, in *absolute* terms, and (2) we showed that accurate steady-state values in *relative* terms can be achieved by applying a near-identity, quasilocal memory-dressing transformation to the observables in question [Eqs. (7)-(10)]. The transformation is only needed for current-like observables with support close to regions connected to baths.

Even for situations where the memory-dressing transformation is needed, the advantageous characteristics of the ULE remain intact. The transformation is only applied *after* evolving the system with the ULE until it reaches its steady state. When applied, the transformation only induces a small, bounded correction to the state or observables. As a result, the procedure remains stable and solvable with stochastic evolution methods (and is hence parallelizable and efficient). The residual deviations are comparable to those expected for the Bloch-Redfield equation (BRE), while avoiding the potential instabilities of the BRE and enabling the use of efficient computational schemes as mentioned above (see, e.g., Ref. [46], where extensive benchmarking was recently performed for a dissipative harmonic oscillator, albeit without the memory-dressing transformation.)

Our results facilitate accurate computation of non-equilibrium currents in the weak-coupling limit via Lindblad equations, ensuring thermodynamic consistency and local conservation laws. Thereby, we demonstrated how to overcome the fundamental limitations intrinsic to any Lindblad equation that were pointed out in Refs. [19, 34].

Important future directions will be to obtain tighter error bounds and to extend the proven regime of validity of the ULE, e.g., by formulating conditions in terms of the spectral range of the system [15]. Other interesting directions involve extending our bounds on steady-state deviations to driven quantum systems, and exploring routes to computing nonequilibrium currents which circumvent the memory dressing transformation. More broadly, our results enable systematic studies of mixed coherent/incoherent evolution in complex quantum sys-

tems, relevant, e.g., for characterizing coherences in noisy devices for quantum information processing.

Acknowledgments — We would like to thank A. Dhar, G. Kirsanskas, M. Kulkarni, M. Leijnse, A. Purkayastha, and D. Tupkary for helpful and clarifying discussions and for pointing out the limitations of the ULE (and Lindblad equations in general), which we address in the present work. F.N. and M.R. gratefully acknowledge the support of Villum Foundation, the European Research Council (ERC) under the European Union Horizon 2020 Research and Innovation Programme (Grant Agreement No. 678862), and CRC 183 of the Deutsche Forschungsgemeinschaft. M. R. is further grateful to the Brown Investigator Award, a program of the Brown Science Foundation, the University of Washington College of Arts and Sciences, and the Kenneth K. Young Memorial Professorship for support. F.N. acknowledges support from the U.S. Department of Energy, Office of Science, Basic Energy Sciences under award DE-SC0019166, the Simons Foundation under award 623768. The work presented here is supported by the Carlsberg Foundation, grant CF22-0727.

Appendix A: Expressions for $\mathcal{V}$

Here we provide an explicit expression for the superoperator $\delta\mathcal{V}$ which enters in the memory dressing transformation. We first show how $\delta\mathcal{V}$ in Eq. (10) is obtained from the corresponding expression given in Ref. [14]. Subsequently (for cases with time-independent Hamiltonians) we provide complementary expressions for $\delta\mathcal{V}$ in terms of the eigenbasis of the Hamiltonian (Sec. A 1) and in terms of an iterative expansion using nested commutators with the Hamiltonian (Sec. A 2). The latter expression may be used in cases where diagonalization of the Hamiltonian is not feasible.

Ref. [14] defines the dressing transformation in the interaction picture, i.e., in the rotating frame where the state of the system is given by $\tilde{\rho}(t) = e^{-iH_S t}\rho(t)e^{iH_S t}$. In this frame, the transformation is given by the $\tilde{V}(t) = 1 + \delta\tilde{\mathcal{V}}(t)$, where the action of $\delta\tilde{\mathcal{V}}(t)$ on a generic Hermitian operator $\mathcal{O}$ is given by

$$\delta\tilde{\mathcal{V}}(t)[\mathcal{O}] = \int_{-\infty}^{\infty} da \int_{-\infty}^{\infty} db\,[\theta(a-t) - \theta(b-t)]\mathcal{G}(a,b)[\rho]. \tag{A1}$$

Here $\mathcal{G}(a,b)$ is a superoperator

$$\mathcal{G}(a,b)[\mathcal{O}] = -\gamma \int_{-\infty}^{a} dc\, g^*(a-b)g^*(b-c)[\tilde{X}(a), \mathcal{O}\tilde{X}(c)] + \text{h.c.}. \tag{A2}$$

Thus we may write

$$\delta\tilde{\mathcal{V}}(t)[\mathcal{O}] = \gamma \int_{-\infty}^{\infty} da \int_{-\infty}^{\infty} dc\,[\tilde{X}(a), \mathcal{O}\tilde{X}(c)] f(a-t, c-t) + \text{h.c.}, \tag{A3}$$

with

$$f(t,t') \equiv \int_{-\infty}^{\infty} db\, g^*(t-b)g^*(b-t')\theta(b-t')[\theta(t) - \theta(b)]. \tag{A4}$$

[See below Eq. (10) in the main text]. When H_S is time-independent, the Schrödinger picture version of $\delta\tilde{\mathcal{V}}$ can be obtained by setting $t = 0$: $\delta\mathcal{V} = \delta\tilde{\mathcal{V}}(0)$. Doing this above yields the result quoted in Eq. (10).

1. Expression for $\mathcal{V}$ in energy eigenbasis

When H_S is time-independent we can conveniently express $\mathcal{V}$ in terms of the energy eigenbasis: writing $\tilde{X}(t) = \sum_{mn} X_{mn} e^{-i\omega_{mn}t}$, where $\omega_{mn} = E_m - E_n$, $X_{mn} \equiv |m\rangle\langle m|X|n\rangle\langle n|$, and $H_S|n\rangle = E_n|n\rangle$, gives us

$$\delta\mathcal{V}[\mathcal{O}] = \sum_{m,n,k,l} [X_{mn}, \mathcal{O}X_{kl}^\dagger] c_{mn;kl} + \text{h.c.}, \tag{A5}$$

with $c_{mn;kl} = 4\pi^2 f(-\omega_{mn}, \omega_{kl})$. Here $f(\omega,\omega') = \frac{1}{4\pi^2}\int_{-\infty}^{\infty} dt \int_{-\infty}^{\infty} dt' e^{i\omega t} e^{i\omega' t'} f(t,t')$ denotes the Fourier transform of $f(t,t')$. A straightforward evaluation of the Fourier transform yields

$$c_{mn;kl} = 2\pi\gamma \int_{-\infty}^{\infty} dq\, \frac{g(q)[g(q) - g(q + \omega_{mn} - \omega_{kl})]}{(\omega_{mn} - \omega_{kl})(q - \omega_{mn} - i0^+)}, \tag{A6}$$

where, for $\omega_{mn} = \omega_{kl}$, the integrand should be evaluated using L'Hospital's rule.

2. Expression of $\mathcal{V}$ in terms of commutator expansion

In cases where diagonalization of the Hamiltonian is not feasible, $\mathcal{V}$ can be computed using an iterative series expansion akin to the one provided for the jump operator in Ref. [14]. We review this expansion for the case of a single bath and a time-independent Hamiltonian, while noting that our results can be extended to multiple baths and time-dependent Hamiltonians. Our first step is to write an expansion for the interaction picture operator $\tilde{X}(t)$:

$$\tilde{X}(t) = \sum_{n=0}^{\infty} \frac{X^{(n)} t^n}{n!} + \text{h.c.}, \quad X^{(n)} = -i[H_S, X^{(n-1)}]. \tag{A7}$$

Here $X^{(n)}$ is the operator obtained from X after n commutation operations with $-iH_S$, where we define $X^{(0)} \equiv X$. Using this expression in the definition of $\mathcal{V}$ [Eq. (10) of the main text] yields

$$\mathcal{V}[\mathcal{O}] = \gamma \sum_{m,n=0}^{\infty} [X^{(m)}, \mathcal{O} X^{(n)}] K_{mn} + \text{h.c.}, \quad K_{mn} \equiv \frac{1}{m!n!} \int_{-\infty}^{\infty} dt \int_{-\infty}^{\infty} dt'\, f(t,t') t^m t'^n. \tag{A8}$$

Referring back to Eq. (A1) with t set to zero (to obtain $\mathcal{V}$ in the Schrödinger picture), and noting that $\mathcal{G}(a,b)$ decays to zero with $|a|, |b|$, we see that $\mathcal{V}$ itself can be computed with a temporal cutoff with an error that goes to zero as the cutoff is increased. For any finite value of the cutoff, the corresponding integrals in Eq. (A8) are finite, and the sum converges. The coefficients $\{K_{mn}\}$ are inexpensive to compute and depend only on the bath jump correlator (but not on any details of the system). Thus the expression in Eq. (A1) provides a viable way to calculate $\mathcal{V}$ to good accuracy for systems where exact diagonalization is not feasible.

Appendix B: Relationship between $\bar{\rho}_{\text{ULE}}$ and $\bar{\rho}'_{\text{exact}}$

Here we establish that $\bar{\rho}'_{\text{exact}} = \bar{\rho}_{\text{ULE}} - \mathcal{L}_{\text{ULE}}^{-1}[\bar{\xi}]$, as quoted in Eq. (13) in the main text. As our starting point, we write a formal solution of Eq. (8) of the main text as

$$\rho'(t) = e^{\mathcal{L}_{\text{ULE}} t}[\rho'(0)] + \int_0^t ds\, e^{\mathcal{L}_{\text{ULE}}(t-s)}[\xi(s)]. \tag{B1}$$

We obtain the exact steady state of the system (in the memory-dressed frame) by taking the $t \to \infty$ limit above: $\lim_{t\to\infty} \rho'(t) = \bar{\rho}'_{\text{exact}}$.

To compute the $t \to \infty$ limit on the right-hand side, we consider the eigendecomposition of $\mathcal{L}_{\text{ULE}}$. Due to its Lindblad form and our assumption of a unique steady state, the superoperator $\mathcal{L}_{\text{ULE}}$ has a single vanishing eigenvalue, while all other eigenvalues have strictly negative real parts. The left and right eigenvectors corresponding to the vanishing eigenvalue are the identity operator and $\bar{\rho}_{\text{ULE}}$, respectively. In particular, the definition of $\bar{\rho}_{\text{ULE}}$ implies $\mathcal{L}_{\text{ULE}}[\bar{\rho}_{\text{ULE}}] = 0$, resulting in

$$\lim_{t\to\infty} e^{\mathcal{L}_{\text{ULE}} t}[\mathcal{O}] = \text{Tr}[\mathcal{O}]\, \bar{\rho}_{\text{ULE}}. \tag{B2}$$

Since $\text{Tr}[\rho'] = 1$, we thus conclude $\lim_{t\to\infty} e^{\mathcal{L}_{\text{ULE}} t}[\rho'(0)] = \bar{\rho}_{\text{ULE}}$. On the other hand, Eq. (8) of the main text implies that $\text{Tr}[\xi(t)] = 0$; hence $e^{\mathcal{L}_{\text{ULE}}(t-s)}[\xi(s)]$ must decay exponentially with $t - s$. Taking the limit $t \to \infty$ in Eq. (B1) hence gives

$$\bar{\rho}'_{\text{exact}} = \bar{\rho}_{\text{ULE}} - \mathcal{L}_{\text{ULE}}^{-1}[\bar{\xi}], \tag{B3}$$

where $\mathcal{L}_{\text{ULE}}^{-1}[\bar{\xi}] \equiv -\int_0^\infty ds\, e^{\mathcal{L}_{\text{ULE}} s} \bar{\xi}$ is finite because $\bar{\xi}$ is traceless. This is the result we wished to establish.

Appendix C: Scaling of $C_{\mathcal{O}}$

Here we show that the dimensionless constant $C_{\mathcal{O}}$ [first appearing in Eq. (14) of the main text] is generically finite in the limit $\Gamma \to 0$. To this end, we recall the definition of $C_{\mathcal{O}}$:

$$C_{\mathcal{O}} = \frac{2\Gamma \| \mathcal{L}_{\text{ULE}}^{\dagger -1}[\mathcal{O}' - \langle \mathcal{O}' \rangle_{\text{ULE}}] \|}{|\langle \bar{\mathcal{O}}' \rangle_{\text{ULE}}|}. \tag{C1}$$

In the following, we use $\Theta(\Gamma^n)$ to indicate quantities that scale as Γ^n in the limit of small Γ. Likewise, we use $O(\Gamma^n)$ to indicate quantities that scale as Γ^n or slower in the same limit. Our goal is to show that $C_{\mathcal{O}} = O(\Gamma^0)$ for generic operators $\mathcal{O}$.

We first consider the case $\mathcal{O} = S$ where $\langle S \rangle_{\text{ULE}}$ is nonzero in the limit $\Gamma \to 0$. Since we assume the system to have a unique steady state, $\mathcal{L}_{\text{ULE}}^\dagger$ has a single vanishing eigenvalue with corresponding left eigenvector $\bar{\rho}_{\text{ULE}}$; all other eigenvalues either scale as $\Theta(\Gamma)$ or $\Theta(\Gamma^0)$. Thus, for any (Γ-independent) operator $\mathcal{M}$ that is orthogonal to $\bar{\rho}_{\text{ULE}}$ (in the sense of the Hilbert-Schmidt inner product), we infer that $\mathcal{L}_{\text{ULE}}^{\dagger -1}[\mathcal{M}] = O(\Gamma^{-1})$. Since $S' - \langle S' \rangle_{\text{ULE}}$ by definition has zero expectation value in the ULE steady state and is hence orthogonal to $\bar{\rho}_{\text{ULE}}$, we have $\mathcal{L}_{\text{ULE}}^{\dagger -1}[S' - \langle S' \rangle_{\text{ULE}}] = O(\Gamma^{-1})$. Using this in Eq. (C1), we conclude that $C_S = O(\Gamma^0)$ for observables with finite expectation values in the limit $\Gamma \to 0$, i.e., with $\lim_{\Gamma\to 0} \langle S' \rangle_{\text{ULE}} \neq 0$.

Next, we consider the case $\mathcal{O} = I$, where I has vanishing steady-state value in the limit $\Gamma \to 0$. Since $\lim_{\Gamma\to 0} \bar{\rho}'$ is diagonal in the eigenbasis of the Hamiltonian [14], there are two classes of operators for which

$\lim_{\Gamma\to 0}\langle\mathcal{O}'\rangle_{\rm ULE}=0$: the first class are operators whose diagonal matrix elements vanish in the eigenbasis of $H_{\mathcal{S}}$. The second class of operators are those that have nonzero diagonal elements in the eigenbasis of $H_{\mathcal{S}}$, but whose combination of diagonal elements nevertheless causes $\mathcal{O}$ to be orthogonal to $\bar{\rho}_{\rm ULE}$. For the latter class of operators, $C_{\mathcal{O}}$ can be infinite. However, the vanishing steady-state value of these operators requires fine-tuning of the system and bath parameters – the operator will generically acquire nonzero steady-state values under perturbations of the bath parameters (such as temperature or chemical potential) or system-bath coupling. We hence expect this case to be non-generic.

Operators whose diagonal matrix elements vanish in the eigenbasis of the Hamiltonian include many physically relevant quantities, such as the total currents of conserved quantities and, in cases of Hamiltonians with time-reversal symmetry, current densities. For this class of operators, we can write

$$I=-i[H_{\mathcal{S}},Q], \tag{C2}$$

for some finite operator Q [48]. The magnon current $I_{n+1,n}$ for the spin chain we consider in the main text can for example be written in the form above with $Q=\sum_{k=1}^{n}\sigma_k^z$ (i.e., with Q measuring the total z-component of spin on sites $1\dots n$). We now use the above property to infer the scaling behavior of C_I.

First, we rewrite Eq. (C2) as $I=\mathcal{L}^\dagger_{\rm ULE}[Q]-\mathcal{D}^\dagger_{\rm ULE}[Q]$, where $\mathcal{D}_{\rm ULE}$ denotes the bath-induced component of the ULE Liouvillian (including the Lamb shift). Writing $\mathcal{V}^{\dagger-1}[I]=I+\left(\frac{1}{1+\delta\mathcal{V}^\dagger}-1\right)[I]$, and using $I'=\mathcal{V}^{\dagger-1}[I]$, we thus have

$$I'=\mathcal{L}^\dagger_{\rm ULE}[Q]+R, \tag{C3}$$

with

$$R=-\mathcal{D}^\dagger_{\rm ULE}[Q]+\left(\frac{1}{1+\delta\mathcal{V}^\dagger}-1\right)[I]. \tag{C4}$$

We now note that $\mathcal{L}_{\rm ULE}[\bar{\rho}_{\rm ULE}]=0$, implying $\mathrm{Tr}(\bar{\rho}_{\rm ULE}\mathcal{L}^\dagger_{\rm ULE}[Q])=0$. Using this relation with Eq. (C3) and the definition $\langle I'\rangle_{\rm ULE}=\mathrm{Tr}[\bar{\rho}_{\rm ULE}\frac{1}{1+\delta\mathcal{V}^\dagger}I]$, we find

$$\langle I'\rangle_{\rm ULE}=\mathrm{Tr}[\bar{\rho}_{\rm ULE}R]. \tag{C5}$$

To infer the scaling behavior of R, we first use $\mathcal{D}^\dagger_{\rm ULE}[Q]=\Theta(\Gamma)$ [14]. Moreover, since $\|\delta\mathcal{V}\|\le\Gamma\tau$, we have $\left((1+\delta\mathcal{V}^\dagger)^{-1}-1\right)[I]=\Theta(\Gamma)$. Thus $R=\Theta(\Gamma)$, implying

$$\langle I'\rangle_{\rm ULE}=\Theta(\Gamma). \tag{C6}$$

This demonstrates that $\lim_{\Gamma\to 0}\langle\bar{A}\rangle=0$ for operators with vanishing diagonal matrix elements in the eigenbasis of $H_{\mathcal{S}}$, as we inferred above.

We now show that $\mathcal{L}^{\dagger-1}[I'-\langle I'\rangle_{\rm ULE}]=\Theta(\Gamma^0)$ for operators that can be written in the form in Eq. (C2). Using Eq. (C3), we first note that

$$\mathcal{L}^{\dagger-1}_{\rm ULE}[I'-\langle I'\rangle_{\rm ULE}]=Q+\mathcal{L}^{\dagger-1}_{\rm ULE}[R-\langle I'\rangle_{\rm ULE}]. \tag{C7}$$

To analyze the second term on the right hand side of this expression, we note two important facts. First, since $\langle I'\rangle_{\rm ULE}=\mathrm{Tr}[\bar{\rho}_{\rm ULE}R]$ [see Eq. (C5)], $R-\langle I'\rangle_{\rm ULE}$ is orthogonal to $\bar{\rho}_{\rm ULE}$. Moreover, according to the discussion above, $R-\langle I'\rangle_{\rm ULE}=\Theta(\Gamma)$. Therefore $\mathcal{L}^{\dagger-1}_{\rm ULE}[R-\langle I'\rangle_{\rm ULE}]=\Theta(\Gamma^0)$. Using $Q=\Theta(\Gamma^0)$, we find

$$\|\mathcal{L}^{\dagger-1}[I'-\langle I'\rangle_{\rm ULE}]\|=\Theta(\Gamma^0). \tag{C8}$$

Combining this with $\langle\bar{I}'\rangle_{\rm ULE}=\Theta(\Gamma)$ in Eq. (C1), we conclude C_I is finite in the limit $\Gamma\to 0$.

Appendix D: Steady-state value of magnetization

Here we provide data for the steady-state values of magnetization on each site, $\{\sigma_n^z\}$, for the 9-site spin chain model considered in the main text. In Fig. 3 we show the steady-state values of the magnetization obtained with (orange) and without (blue) applying the correction from the memory dressing transformation, $\langle\sigma_n^{z\prime}\rangle_{\rm ULE}$, and $\langle\sigma_n^z\rangle_{\rm ULE}$, respectively. As for the computation of the bond current in the main text, we apply the inverse memory-dressing transformation through expansion to first order, setting $\mathcal{V}^{-1}\approx(1-\delta\mathcal{V})$ to compute $\langle\sigma_n^{z\prime}\rangle_{\rm ULE}$. The two data sets coincide up to negligible relative corrections, as we expected due to the finite value of $\langle\sigma_n^z\rangle_{\rm ULE}$ in the weak coupling limit (see main text).

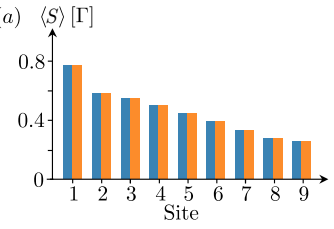

FIG. 3. Steady-state values of the undressed ($\{\langle\sigma_n^z\rangle_{\rm ULE}\}$, blue) and dressed ($\{\langle\sigma_n^{z\prime}\rangle_{\rm ULE}\}$, orange) on-site magnetizations in the spin-chain model considered in the main text.

[1] P. A. M. Dirac, The quantum theory of the emission and absorption of radiation, Proc. R. Soc. Lond. **114**, 243 (1927).

[2] S. Nakajima, On Quantum Theory of Transport Phenomena: Steady Diffusion, Progress of Theoretical Physics **20**, 948 (1958).

[3] R. Zwanzig, Ensemble method in the theory of irreversibility, The Journal of Chemical Physics **33**, 1338 (1960).

[4] A. G. Redfield, The theory of relaxation processes, Advances in Magnetic and Optical Resonance **1**, 1 (1965).

[5] E. B. Davies, Markovian master equations, Comm. Math. Phys. **39**, 91 (1974).

[6] H. P. Breuer and F. Petruccione, *The theory of open quantum systems* (Oxford University Press, Great Clarendon Street, 2002).

[7] L. M. Sieberer, M. Buchhold, and S. Diehl, Keldysh field theory for driven open quantum systems, Reports on Progress in Physics **79**, 096001 (2016).

[8] G. Kiršanskas, M. Franckié, and A. Wacker, Phenomenological position and energy resolving Lindblad approach to quantum kinetics, Phys. Rev. B **97**, 035432 (2018).

[9] A. Strathearn, P. Kirton, D. Kilda, J. Keeling, and B. W. Lovett, Efficient non-markovian quantum dynamics using time-evolving matrix product operators, Nature Communications **9**, 3322 (2018).

[10] F. Nathan, I. Martin, and G. Refael, Topological frequency conversion in a driven dissipative quantum cavity, Physical Review B **99**, 094311 (2019).

[11] E. Kleinherbers, N. Szpak, J. König, and R. Schützhold, Relaxation dynamics in a Hubbard dimer coupled to fermionic baths: Phenomenological description and its microscopic foundation, Phys. Rev. B **101**, 125131 (2020).

[12] G. McCauley, B. Cruikshank, D. I. Bondar, and K. Jacobs, Accurate Lindblad-form master equation for weakly damped quantum systems across all regimes, npj Quantum Information **6**, 74 (2020).

[13] E. Mozgunov and D. Lidar, Completely positive master equation for arbitrary driving and small level spacing, Quantum **4**, 227 (2020).

[14] F. Nathan and M. S. Rudner, Universal Lindblad equation for open quantum systems, Phys. Rev. B **102**, 115109 (2020).

[15] D. Davidović, Geometric-arithmetic master equation in large and fast open quantum systems, Journal of Physics A: Mathematical and Theoretical **55**, 455301 (2022).

[16] A. D. Somoza, O. Marty, J. Lim, S. F. Huelga, and M. B. Plenio, Dissipation-assisted matrix product factorization, Phys. Rev. Lett. **123**, 100502 (2019).

[17] T. Becker, L.-N. Wu, and A. Eckardt, Lindbladian approximation beyond ultraweak coupling, Phys. Rev. E **104**, 014110 (2021).

[18] A. Lerose, M. Sonner, and D. A. Abanin, Influence Matrix Approach to Many-Body Floquet Dynamics, Phys. Rev. X **11**, 021040 (2021).

[19] P. P. Potts, A. A. S. Kalaee, and A. Wacker, A thermodynamically consistent Markovian master equation beyond the secular approximation, New Journal of Physics **23**, 123013 (2021).

[20] T. Mori, Floquet states in open quantum systems, Annual Review of Condensed Matter Physics **14**, 35 (2023).

[21] G. Lindblad, On the generators of quantum dynamical semigroups, Communications in Mathematical Physics **48**, 119 (1976).

[22] V. Gorini, A. Kossakowski, and E. C. G. Sudarshan, Completely positive dynamical semigroups of N-level systems, Journal of Mathematical Physics **17**, 821 (1976).

[23] J. Dalibard, Y. Castin, and K. Mølmer, Wave-function approach to dissipative processes in quantum optics, Phys. Rev. Lett. **68**, 580 (1992).

[24] H. Carmichael, *An open systems approach to quantum optics* (Springer, 1993).

[25] G. Kurizki, P. Bertet, Y. Kubo, K. Mølmer, D. Petrosyan, P. Rabl, and J. Schmiedmayer, Quantum technologies with hybrid systems, Proceedings of the National Academy of Sciences **112**, 3866 (2015), publisher: Proceedings of the National Academy of Sciences.

[26] T. Oka and S. Kitamura, Floquet engineering of quantum materials, Annual Review of Condensed Matter Physics **10**, 387 (2019).

[27] A. Browaeys and T. Lahaye, Many-body physics with individually controlled Rydberg atoms, Nature Physics **16**, 132 (2020), number: 2 Publisher: Nature Publishing Group.

[28] M. Kjaergaard, M. E. Schwartz, J. Braumüller, P. Krantz, J. I.-J. Wang, S. Gustavsson, and W. D. Oliver, Superconducting qubits: Current state of play, Annual Review of Condensed Matter Physics **11**, 369 (2020).

[29] F. Nathan, *Topological Phenomena in Periodically Driven Systems*, Ph.D. thesis, University of Copenhagen (2018).

[30] T. Maimbourg, D. M. Basko, M. Holzmann, and A. Rosso, Bath-induced zeno localization in driven many-body quantum systems, Phys. Rev. Lett. **126**, 120603 (2021).

[31] J. Mielke, J. R. Petta, and G. Burkard, Nuclear spin readout in a cavity-coupled hybrid quantum dot-donor system, PRX Quantum **2**, 020347 (2021).

[32] M. A. *et al* (Microsoft Azure Quantum), Interferometric single-shot parity measurement in an inas-al hybrid device (2024), arXiv:2401.09549 [cond-mat.mes-hall].

[33] F. Garcia-Gaitan and B. K. Nikolic, Fate of entanglement in magnetism under lindbladian or non-markovian dynamics and conditions for their transition to landau-lifshitz-gilbert classical dynamics (2024), arXiv:2303.17596 [cond-mat.str-el].

[34] D. Tupkary, A. Dhar, M. Kulkarni, and A. Purkayastha, Fundamental limitations in Lindblad descriptions of systems weakly coupled to baths, Phys. Rev. A **105**, 032208 (2022).

[35] A nonzero expectation value can be absorbed into H_S after appropriate redefinition of B. If X has an unbounded spectrum, an appropriate cutoff for its eigenvalues has to be implemented.

[36] We consider systems which have a unique steady state; cases with multiple fixed points, such as systems that support spontaneous symmetry breaking or local integrals of motion, are left for future studies.

[37] In Ref. [14], the bound was established for the spectral norm; however the same arguments are valid for the trace norm.

[38] The Bloch-Redfield Liouvillian is given by $\mathcal{L}_{\rm BR}[\rho] \equiv -i[H_S,\rho] - \sum_{\alpha\beta}\gamma\int_0^\infty dt\big(J_{\alpha\beta}(t)\big[X_\alpha, e^{iH_St}X_\beta e^{-iH_St}\rho\big] + \text{h.c.}\big)$.

[39] This follows from the property of $\mathcal{V}$ above, along with $\|\xi_{\rm BR}\| \le \Gamma^2\tau$, $\|\partial_t\rho - i[\rho,H_S]\| \le \Gamma/2$, and $\|\mathcal{V}-\mathbf{1}\|_{\rm SO} \le \Gamma\tau$ (see below).

[40] Here $\mathcal{V}^\dagger$ denotes the adjoint of $\mathcal{V}$ with respect to the Hilbert-Schmidt inner product, $(A, B) \equiv \mathrm{Tr}[A^\dagger B]$.

[41] One can construct operators with nonvanishing diagonal matrix elements in the energy basis, whose expectation values vanish in the limit $\Gamma \to 0$ (such that the relative deviation does not scale to zero with Γ). We expect that such observables are non-generic and require fine-tuning.

[42] This result follows from $\langle\mathcal{O}\rangle_{\mathrm{ULE}} - \langle\mathcal{O}'\rangle_{\mathrm{ULE}} = \mathrm{Tr}\big[\mathcal{O}\big(1-\mathcal{V}^{-1}\big)[\bar{\rho}_{\mathrm{ULE}}]\big]$, and from using $\|\delta\mathcal{V}\| \leq \Gamma\tau$, and $\|\bar{\rho}_{\mathrm{ULE}}\| = 1$.

[43] C. Gardiner and P. Zoller, *Quantum Noise* (Springer-Verlag Berlin Heidelberg, 2004).

[44] We emphasize that uniformity of the bond currents alone does not imply that the value of current is accurate. For example, while the BR approach ensures uniformity of the current by construction, its accuracy is guaranteed only in the weak coupling limit [49].

[45] We apply the inverse frame transformation through expansion to first order, setting $\mathcal{V}^{-1} \approx 1 - \delta\mathcal{V}$.

[46] C. S. T. Breuer, T. Becker, and A. Eckardt, Benchmarking quantum master equations beyond ultraweak coupling (2024), arXiv:2403.08320 [quant-ph].

[47] This expression follows from Eqs. (C2), (C4), and (C7) in Ref. [14], when using that $\theta(a)\theta(-b) - \theta(b)\theta(-a) = \theta(a) - \theta(b)$.

[48] Note that Q is not uniquely defined, since adding a term diagonal in the eigenbasis of H_S to Q will not change I.

[49] Specifically, $|\langle\mathcal{O}\rangle_{\mathrm{exact}} - \langle\mathcal{O}\rangle_{\mathrm{BR}}| \leq \Gamma\tau C_{\mathcal{O}}|\langle\bar{\mathcal{O}}\rangle_{\mathrm{BR}}|$, with $C'_{\mathcal{O}} \equiv \Gamma\|(\mathcal{L}^\dagger_{\mathrm{BR}})^{-1}[\mathcal{O} - \langle\mathcal{O}\rangle_{\mathrm{BR}}]\|/\langle\mathcal{O}\rangle_{\mathrm{BR}}$, where $\langle\mathcal{O}\rangle_{\mathrm{BR}}$ denotes the expectation value of $\mathcal{O}$ in the steady state of the BR equation and $\mathcal{L}_{\mathrm{BR}}$ denotes the Bloch-Redfield Liouvillian. For small Γ, $C'_{\mathcal{O}}$ follows similar scaling behavior to that of $C_{\mathcal{O}}$ as described in the SOM [50].

[50] See Supplementary Online Material for: A) exlplicit expressions for the frame transformation $\mathcal{V}$, B) explicit derivation of the result $\bar{\rho}'_{\mathrm{exact}} = \bar{\rho}_{\mathrm{ULE}} + \mathcal{L}^{-1}_{\mathrm{ULE}}[\bar{\xi}]$, C) Data showing the steady-state value of magnetization in the simulated spin-chain model, and D) analysis of the small-Γ behavior of $C_{\mathcal{O}}$.